

Out-of-plane Auxeticity in Sintered Fibre Network Mats

Suresh Neelakantan¹, Jin-Chong Tan², Athina E Markaki¹

¹*Department of Engineering, University of Cambridge, Trumpington Street,
Cambridge CB2 1PZ, UK*

²*Department of Engineering Science, University of Oxford, Parks Road,
Oxford, OX1 3PJ, UK*

Abstract

Fibre network mats composed of stainless steel exhibit an unusually large out-of-plane auxeticity (i.e. high negative Poisson's ratio ν) when subjected to in-plane tensile loading. *In situ* observations in a scanning electron microscope suggest that this is attributable to fibre segment straightening. An investigation was carried out on the effects of fibre volume fraction and network thickness on the auxetic response. Weak inter-layer bonding, high fibre content and low network thickness were found to amplify the auxetic effect.

Keywords: porous material; fibers; tension test; stainless steels; Poisson's ratio

1 Conventional materials contract laterally when stretched along their length. By
2 contrast, auxetic materials exhibit a dilatational behaviour, i.e. they expand in the
3 transverse direction when stretched, and are therefore characterised by negative values
4 of the Poisson's ratio ($\nu = - \text{transverse strain} / \text{axial strain}$) [1-3]. Auxetic materials
5 are of interest due to their potential to achieve enhancement of material properties
6 related to Poisson's ratio [1, 4-7]. For 3D isotropic materials, the numerical limits for
7 Poisson's ratio ν are set by -1 and 0.5, arising from the relationship between the
8 Poisson's ratio, the bulk K and shear G moduli [6, 8]. However, for anisotropic
9 materials, these are independent elastic constants, so strong auxetic effects are
10 theoretically permissible. A schematic showing the wide range of negative Poisson's
11 ratio measured experimentally for various materials is illustrated in Figure 1. Low
12 auxeticity naturally exists in some single crystals (e.g. sulfide minerals, metals,
13 metalloids and intermetallics) [8-12]. Similar levels of auxeticity have been observed
14 in silicates (α -cristobalite, zeolites) attributed to rotation of "building blocks" [13, 14];
15 cubic metals when stretched in [110] direction [11]; liquid crystalline polymers (eg.
16 carbocyclic-, poly(phenylacetylene)- networks) due to the connectivity between the
17 rigid centre region and the flexible ends of elongated organic molecules [2, 15-17]
18 and skin tissue (cat, cow teat) attributed to their fibrillar structure [18, 19]. Man-made
19 auxetic materials include re-entrant or hinged honeycombs and foams, which exhibit
20 auxeticity due to the unfolding of re-entrant cells [1, 20-23]; microporous polymers
21 (Polytetrafluoroethylene (PTFE), ultra-high molecular weight polyethylene
22 (UHMWPE), Polypropylene (PP)) [2, 24, 25]. These polymers consist of an
23 interconnected network of nodules and fibrils and auxeticity has been attributed to the
24 fibrils causing nodule translation when a load is applied [2, 25-27]. Auxetic effects
25 have also been observed in fibre composites involving the use of auxetic constituents
26 (polymeric or ceramic fibres [28, 29]) or selection of suitable stacking sequences of
27 unidirectional laminae [30-33]. However, high levels of auxeticity in fibre composites
28 have only been achieved by the incorporation of metallic fibre networks [29]. These
29 networks can be used as a stand-alone material [34] or as reinforcement in composites
30 [29]. Such fibre assemblies are highly oriented (fibres oriented mostly in-plane) and
31 are produced by sintering fibres together at crossover points. They are in many
32 respects intermediate between "materials" and "structures".
33
34
35
36
37
38
39
40
41
42
43
44
45
46
47
48
49
50
51
52
53
54
55
56
57
58
59
60
61
62
63
64
65

1 The measured out-of-plane Poisson's ratios of metallic fibre networks mats
2 [29, 34-36] reported to date are summarised in Table 1. Values as negative as -18
3 have been reported. However, the reason for such a large auxeticity has so far not
4 been demonstrated experimentally. This study aims to elucidate the mechanism that
5 causes such a large out-of-plane auxeticity in fibre networks. Herein the effects of
6 fibre volume fraction and mat thickness on the out-of-plane Poisson's ratio have been
7 investigated.

8
9
10
11
12
13 Fibre network plates, made of 316L austenitic stainless steel (N.V. Bekaert
14 S.A., Belgium), were supplied in three different fibre volume fractions f (10, 15 and
15 20 vol%) and three thicknesses, t (1, 2 and 5 mm). The 316L fibres are produced by a
16 bundle drawing process and have a hexagonal cross-sectional shape (diagonal length
17 40 μm). Network plates, made of 444 ferritic stainless steel fibres (Nikko Techno,
18 Japan), have also been considered in this study. The plates are 5 mm thick and contain
19 15 vol% of rectangular ($80 \times 100 \mu\text{m}^2$) 444 fibres, produced by a coil-shaving
20 process. The network plates are processed as follows [35-37]: i) overlapping of
21 individual slender fibres to form fibre webs of fixed density with random planar
22 orientation; ii) stacking few layers of such fibre webs upon one another, compressed
23 and sintered to plates of specific dimensions.

24
25
26
27
28
29
30
31
32
33 *In situ* tensile testing of 316L fibre networks was carried out using a Zeiss Evo
34 LS15 VP model scanning electron microscope in secondary electron mode. A
35 DEBEN[®] tensile stage, equipped with a 5 kN load cell, was mounted in the SEM
36 stage. Rectangular dog-bone tensile specimens were electro-discharge machined from
37 316L network plates according to ASTM E8-11 sub-size specimen standards. The
38 gauge sections were 30 mm long (x direction), 6 mm wide (y direction) and 5 mm
39 thick (z direction). In order to prevent crushing in the grip sections, the ends of the
40 specimens were impregnated by Loctite super glue. To increase the chances of
41 capturing the auxetic mechanism *in situ*, a further region within the sample gauge
42 section, was impregnated with Loctite super glue thereby leaving roughly 9 mm
43 exposure region to the electron beam. All tests were conducted in displacement
44 control mode at a rate of 0.1 mm min^{-1} . The cross-head displacement was measured
45 using an LVDT.

46
47
48
49
50
51
52
53
54
55
56
57 In-plane tensile testing was carried using an Instron testing machine fitted with
58 a 5 kN load cell. Rectangular dog-bone samples were cut out from 316L network
59

1 plates of different thicknesses (1, 2, 5 mm) and 5 mm 444 networks. The in-plane
2 dimensions of the sample gauge sections were identical to those used for *in situ*
3 tensile testing. The displacements in the xz plane were captured using Digital Image
4 Correlation (DIC) and analysed in order to evaluate the out-of-plane Poisson's ratios
5 as described elsewhere [34].
6
7

8
9 A Dynamic Mechanical Analyser (DMA, Triton Technology Ltd) was used to
10 measure the out-of-plane Young's modulus (E_z) of the 316L fibre networks with
11 different fibre volume fractions. The tests were carried out in three-point bending
12 mode, with a 12.5 mm loading span, at 1 Hz frequency and 0.1 mm displacement
13 amplitude. Network beams, measuring 5 mm in thickness and 6 mm in width, were
14 used.
15
16
17
18
19

20 For all experiments (except the *in situ* experiments where a single sample was
21 used), at least 3 tests were carried out for each sample type, from which the average
22 value was taken and standard deviation calculated.
23
24

25 For *in situ* tensile testing, the through-thickness face (xz plane) of the 316L
26 networks was exposed to the electron gun. A region within the sample gauge section,
27 as shown in Figure 2, was identified to continuously monitor *in situ*, while applying
28 an in-plane tensile load on the sample. Figure 2a shows the through-thickness view,
29 with fibres (highlighted in red) appearing inwardly bent. During in-plane loading
30 (0.4% strain), the bent fibres (highlighted in red) were found to straighten up as
31 illustrated in Figure 2b. This is also evident from the video (*click on the video link*
32 *(only for online version) showing the behaviour*), suggesting that fibre straightening
33 or outward bending causes lateral expansion of the sample in the through-thickness
34 direction. The corollary is that, during processing, the through-thickness pressure
35 causes the fibre segments between joints to curve inwards. When the networks are
36 stretched in-plane, the fibres straighten or bend outwards. *In situ* observations suggest
37 that the fibre segments with high radius of curvature (a few mm) are the ones that
38 straightened up compared to those with low radius of curvature.
39
40
41
42
43
44
45
46
47
48
49
50

51 In our previous study [34], the out-of-plane Poisson's ratio was found to
52 become more negative as the fibre volume fraction increases. Figure 3a shows the
53 longitudinal strain ε_x as a function of the out-of-plane strain ε_z of 316L networks with
54 three fibre volume fractions. Given that during sintering the applied compression
55 pressure increases with fibre volume fraction, it can be postulated that fibres at high
56
57
58
59
60
61
62
63
64
65

1 density networks protrude more inwards during processing compared with the low
2 density ones resulting in a larger lateral expansion in response to axial (in-plane)
3 loading. This is in agreement with previously measured mean fibre segment
4 inclination angles [34] obtained from X-ray tomography. Figure 3b shows that the
5 mean fibre segment inclination angles, with respect to the out-of-plane direction (z
6 axis), are somewhat lower for lower fibre content networks, i.e. fibre segments are
7 sitting more in-plane in the 10% networks.
8
9

10
11
12 A further observation is that the inter-layer bonding in these networks is weak
13 causing the networks to continuously expand in the through-thickness direction with
14 increasing load (beyond the elastic region), thereby resulting in intra-laminar cracking
15 and significant through-thickness thickening [34].
16
17

18
19
20 In order to investigate whether the number of inter-layers, i.e. the network
21 thickness, affects the Poisson ratio, in-plane tensile testing was carried out using 316L
22 networks of the same fibre volume fraction but with different plate thicknesses. Figure
23 4a shows the longitudinal strain ε_x versus the out-of-plane strain ε_z for 316L networks
24 with 15% fibre volume fraction. It can be seen that the slopes, representing the out-of-
25 plane Poisson's ratio, become more negative with decreasing plate thickness. As
26 Figure 4b shows, the auxetic effect amplifies (i.e. negative Poisson's value increases)
27 almost exponentially as the thickness of the plate reduces from 5 mm to 1 mm.
28 Assuming that the inter-layer bonding is not changing with network thickness, the
29 observed trend suggests that thin plates, with less inter-layers, can expand more freely
30 in the out-of-plane direction, leading to a more negative Poisson's value as compared
31 to thick plates, which are more constrained by the larger number of inter-fibre layers.
32 This suggests that weak inter-layer bonding plays a role in the auxetic response of
33 these networks.
34
35

36
37
38 Table 2 shows the out-of-plane Young's modulus (E_z) of the networks
39 obtained from DMA testing. Also, shown for comparison, are the in-plane Young's
40 moduli (E_x and E_y) obtained from in-plane tensile testing [34]. As expected, the values
41 are dominated by the dependence on fibre volume fraction, i.e. the Young's moduli
42 increase with increasing fibre volume fraction. The out-of-plane modulus is
43 approximately two orders of magnitudes lower than the corresponding in-plane
44 values. This is unsurprising, as fibres inclined at high θ angles to the vertical will
45 offer low resistance to vertical displacement.
46
47
48
49
50
51
52
53
54
55
56
57
58
59
60
61
62
63
64
65

1
2 In order to further verify that the auxetic behaviour arises by virtue of the
3 network's structure and processing, a different network, made of 444 ferritic stainless
4 steel fibres, was considered. While the sintering conditions are expected to be slightly
5 different (because of the different fibre material), the 444 networks are processed in a
6 similar fashion as 316L networks. However, the 444 fibres have a non-uniform cross-
7 sectional shape (rectangular vs cylindrical for 316L fibre), so in practice the fibres
8 would bend in planes in which they have relatively low moment of inertia. Figure 4c
9 shows the longitudinal strain ε_x versus the out-of-plane strain ε_z , for both 316L and
10 444 networks of the same fibre volume fraction ($f = 15\%$). (Specimen dimensions and
11 experimental parameters were the same as those used for testing 316L networks). It
12 can be seen that similar Poisson's ratios were measured on both networks, suggesting
13 that the out-of-plane auxetic response of the fibre networks mainly arises from the
14 processing method.
15
16
17
18
19
20
21
22
23
24

25 In summary, sintered metallic fibre network mats exhibit a strong out-of-plane auxetic
26 behaviour. The auxetic effect is attributed to fibre straightening (i.e. outward bending)
27 in response to in-plane tensile testing. Fibre kinking is induced during processing due
28 to the applied pressure. The results suggest that weak inter-layer bonding, high fibre
29 content and low network thickness tend to amplify the auxetic effect.
30
31
32
33
34
35

36 This research was supported by the European Research Council (Grant No. 240446).
37 We wish to thank Dr. Kalin Dragnevski at The Laboratory for In-situ Microscopy and
38 Analysis (LIMA) in the Department of Engineering Science, Oxford University for
39 the help in setting up the *in situ* DEBEN experiments.
40
41
42
43
44
45
46
47
48
49
50
51
52
53
54
55
56
57
58
59
60
61
62
63
64
65

References

- [1] R. Lakes, *Science*, 235 (1987) 1038.
- [2] K.E. Evans, M.A. Nkansah, I.J. Hutchinson, S.C. Rogers, *Nature*, 353 (1991) 124.
- [3] R. Lakes, *Advanced Materials*, 5 (1993) 293.
- [4] K.E. Evans, K.L. Alderson, *Engineering Science and Education Journal*, 9 (2000) 148.
- [5] K.E. Evans, A. Alderson, *Advanced Materials*, 12 (2000) 617.
- [6] G.N. Greaves, A.L. Greer, R.S. Lakes, T. Rouxel, *Nature Materials*, 10 (2011) 823.
- [7] Y. Prawoto, *Computational Materials Science*, 58 (2012) 140.
- [8] A.E.H. Love, *A Treatise on the Mathematical Theory of Elasticity*, Second ed., Cambridge University Press, Cambridge, 1906.
- [9] D.J. Gunton, G.A. Saunders, *Journal of Materials Science*, 7 (1972) 1061.
- [10] Y. Li, *Physica Status Solidi (A)*, 38 (1976) 171.
- [11] R.H. Baughman, J.M. Shacklette, A.A. Zakhidov, S. Stafstrom, *Nature*, 392 (1998) 362.
- [12] Z.A.D. Lethbridge, R.I. Walton, A.S.H. Marmier, C.W. Smith, K.E. Evans, *Acta Materialia*, 58 (2010) 6444.
- [13] A. Yeganeh-Haeri, D.J. Weidner, J.B. Parise, *Science*, 257 (1992) 650.
- [14] J.N. Grima, R. Gatt, V. Zammit, J.J. Williams, K.E. Evans, A. Alderson, R.I. Walton, *Journal of Applied Physics*, 101 (2007) 086102.
- [15] R.H. Baughman, D.S. Galvao, *Nature*, 365 (1993) 735.
- [16] J.N. Grima, K.E. Evans, *Chemical Communications*, 36 (2000) 1531.
- [17] C. He, P. Liu, P.J. McMullan, A.C. Griffin, *Physica Status Solidi (B)*, 242 (2005) 576.
- [18] D.R. Veronda, R.A. Westmann, *Journal of Biomechanics*, 3 (1970) 15.
- [19] C. Lees, J.F.V. Vincent, J.E. Hillerton, *Bio-Medical Materials and Engineering*, 1 (1991) 19.
- [20] R.F. Gibson, M.F. Ashby, G.S. Schajer, C.I. Robertson, *Proceedings of The Royal Society of London. Series A, Mathematical and Physical Sciences*, 382 (1982) 25.
- [21] R.F. Almgren, *Journal of Elasticity*, 15 (1985) 427.
- [22] E.A. Friis, R.S. Lakes, J.B. Park, *Journal of Materials Science*, 23 (1988) 4406.
- [23] D. Prall, R.S. Lakes, *International Journal of Mechanical Sciences*, 39 (1997) 305.
- [24] B.D. Caddock, K.E. Evans, *Journal of Physics D: Applied Physics*, 22 (1989) 1877.
- [25] K.L. Alderson, K.E. Evans, *Polymer*, 33 (1992) 4435.

- 1 [26] K.E. Evans, B.D. Caddock, *Journal of Physics D: Applied Physics*, 22 (1989)
2 1883.
- 3 [27] J.N. Grima, R. Caruana-Gauci, D. Attard, R. Gatt, *Proceedings of the Royal*
4 *Society A: Mathematical, Physical and Engineering Sciences*, 468 (2012) 3121.
- 5 [28] R.F. Gibson, *Principles of composite material mechanics*, First ed., McGraw-
6 Hill, New York, 1994.
- 7 [29] S. Jayanty, J. Crowe, L. Berhan, *Physica Status Solidi (B)*, 248 (2011) 73.
- 8 [30] C.T. Herakovich, *Journal of Composite Materials*, 18 (1984) 447.
- 9 [31] J.F. Clarke, R.A. Duckett, P.J. Hine, I.J. Hutchinson, I.M. Ward, *Composites*, 25
10 (1994) 863.
- 11 [32] K.E. Evans, J.P. Donoghue, K.L. Alderson, *Journal of Composite Materials*, 38
12 (2004) 95.
- 13 [33] K.L. Alderson, V.R. Simkins, V.L. Coenen, P.J. Davies, A. Alderson, K.E.
14 Evans, *Physica Status Solidi (B)*, 242 (2005) 509.
- 15 [34] S. Neelakantan, W. Bosbach, J. Woodhouse, A.E. Markaki, *Acta Materialia*, 66
16 (2014) 326.
- 17 [35] F. Delannay, T.W. Clyne, in: J. Banhart, M.F. Ashby, N.A. Fleck (Eds.) *Metal*
18 *Foams and Porous Metal Structures*, MIT-Verlag, 1999, pp. 293-298.
- 19 [36] M. Tatlier, L. Berhan, *Physica Status Solidi (B)*, 246 (2009) 2018.
- 20 [37] R.D. Bruyne, H. Schepeas, I. Lefever, R. Loufeld, in: *United States Patent;*
21 *Patent Number: 4983467*, N.V. Bekaert S.A., Zwevegem, Belgium, 1991.
- 22
23
24
25
26
27
28
29
30
31
32
33
34
35
36
37
38
39
40
41
42
43
44
45
46
47
48
49
50
51
52
53
54
55
56
57
58
59
60
61
62
63
64
65

Figure Captions

1
2 **Figure 1:** Schematic showing the range of negative Poisson's ratio in auxetic
3 materials.

4
5 **Figure 2:** Scanning electron microscopy images of a region in the through-thickness
6 face of the 316L fibre networks ($f = 10\%$) showing fibres (some of them highlighted
7 in red) (a) before and (b) after application of an in-plane tensile load (applied
8 horizontally) corresponding to 0.4% strain.
9

10 **Figure 3:** (a) In-plane longitudinal strain as a function of out-of-plane strain,
11 measured during in-plane tensile testing of 316L fibre networks, for three different
12 fibre volume fractions; (b) Out-of-plane Poisson's ratio plotted as a function of mean
13 fibre inclination angles (with respect to the through-thickness direction), obtained
14 from X-ray tomography [34], for different fibre volume fractions.
15

16 **Figure 4:** (a) In-plane longitudinal strain as a function of out-of-plane strain for 316L
17 fibre networks with $f = 15\%$, with three different plate thicknesses; (b) Experimental
18 dependence on plate thickness of the out-of-plane Poisson's ratio of 316L fibre
19 networks with $f = 15\%$; (c) In-plane longitudinal strain as a function of out-of-plane
20 strain for 316L and 444 fibre networks with $f = 15\%$.
21
22
23
24
25
26
27
28
29
30
31
32
33
34
35
36
37
38
39
40
41
42
43
44
45
46
47
48
49
50
51
52
53
54
55
56
57
58
59
60
61
62
63
64
65

Network thickness t (mm)	Fibre diameter (μm)	Fibre volume fraction f (%)	Out-of-plane Poisson's ratio $-v_{xz}$ (-)	Method for strain measurement	Reference
10	12	20	1.7	Clip-gauge extensometer	[35]
unknown	30	20 – 40	5.4 – 18.6	Laser extensometer	[29]
5	40	10 – 20	5.3 – 10.7	Digital Image Correlation	[34]

Table 1: Negative out-of-plane Poisson's ratio values measured for transversely isotropic metallic fibre networks subjected to in-plane tension. In all studies the fibre material was austenitic stainless steel 316L supplied by N.V. Bekaert, Belgium.

Fibre volume fraction f (%)	Young's modulus (GPa)		
	Out-of-plane	In-plane	
	E_z	E_x	E_y
10	0.0069 ± 0.0011	1.17 ± 0.32	1.13 ± 0.06
15	0.0087 ± 0.0011	2.19 ± 0.11	2.28 ± 0.59
20	0.0094 ± 0.0006	2.51 ± 0.06	3.10 ± 0.86

Table 2: Out-of-plane Young's modulus E_z for 316L fibre networks with different fibre volume fractions, as obtained by DMA testing. Also, shown are the in-plane Young's moduli (E_x and E_y) measured using tensile testing [34]. All measurements were carried out using 5 mm thick plates.

Figure 1
[Click here to download high resolution image](#)

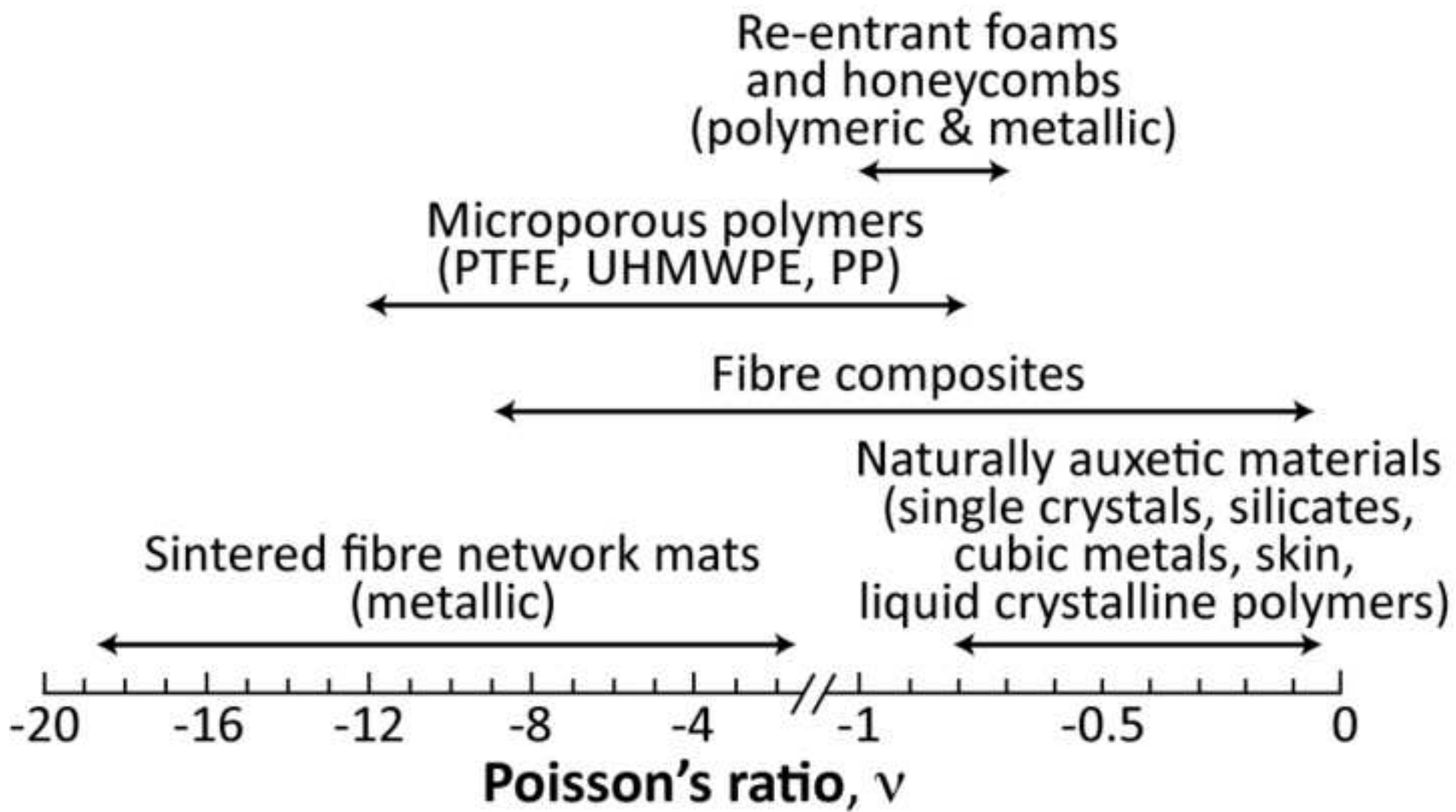


Figure 2
[Click here to download high resolution image](#)

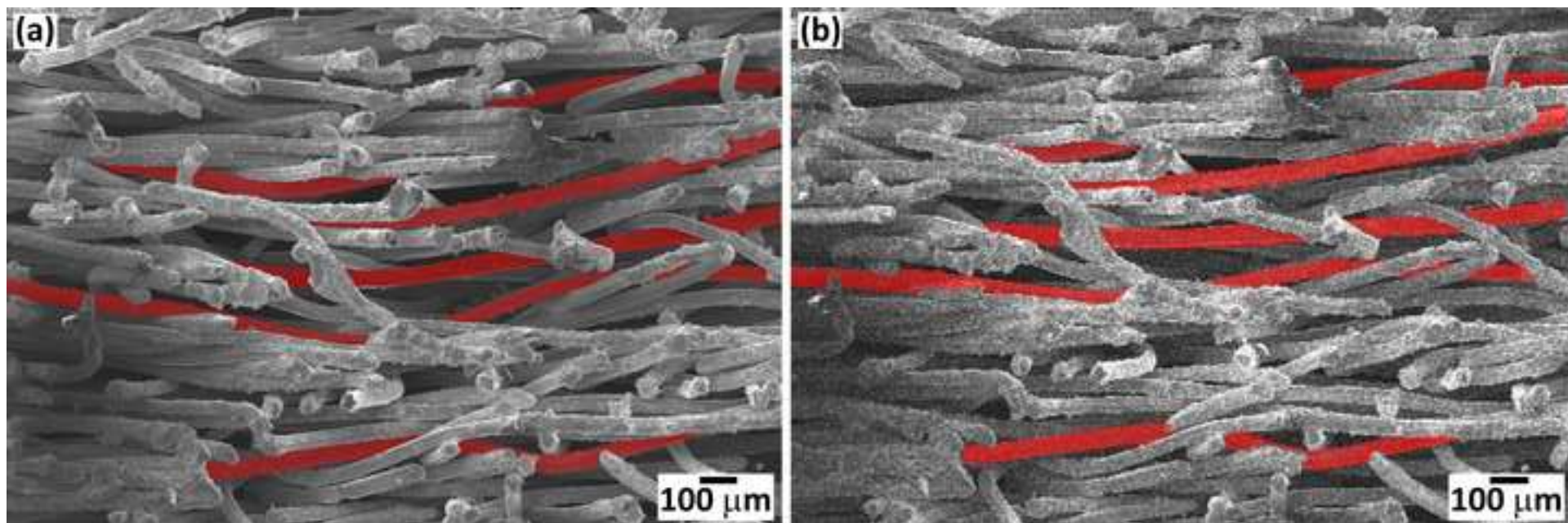


Figure 3
[Click here to download high resolution image](#)

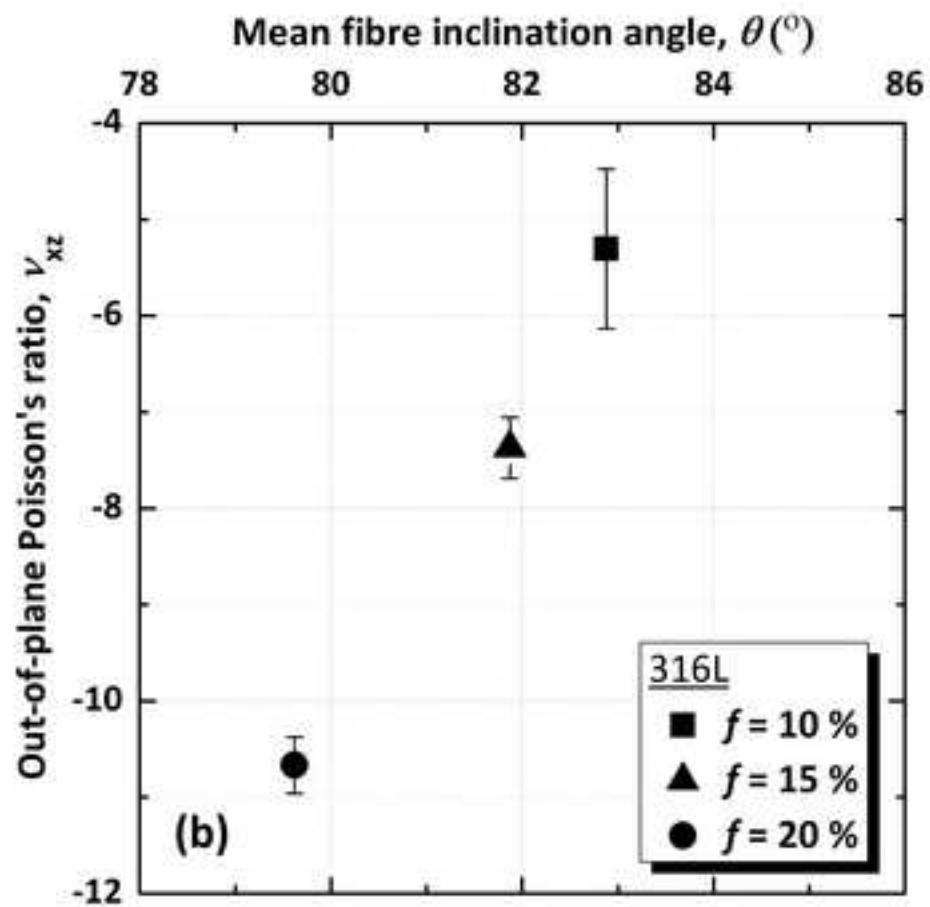
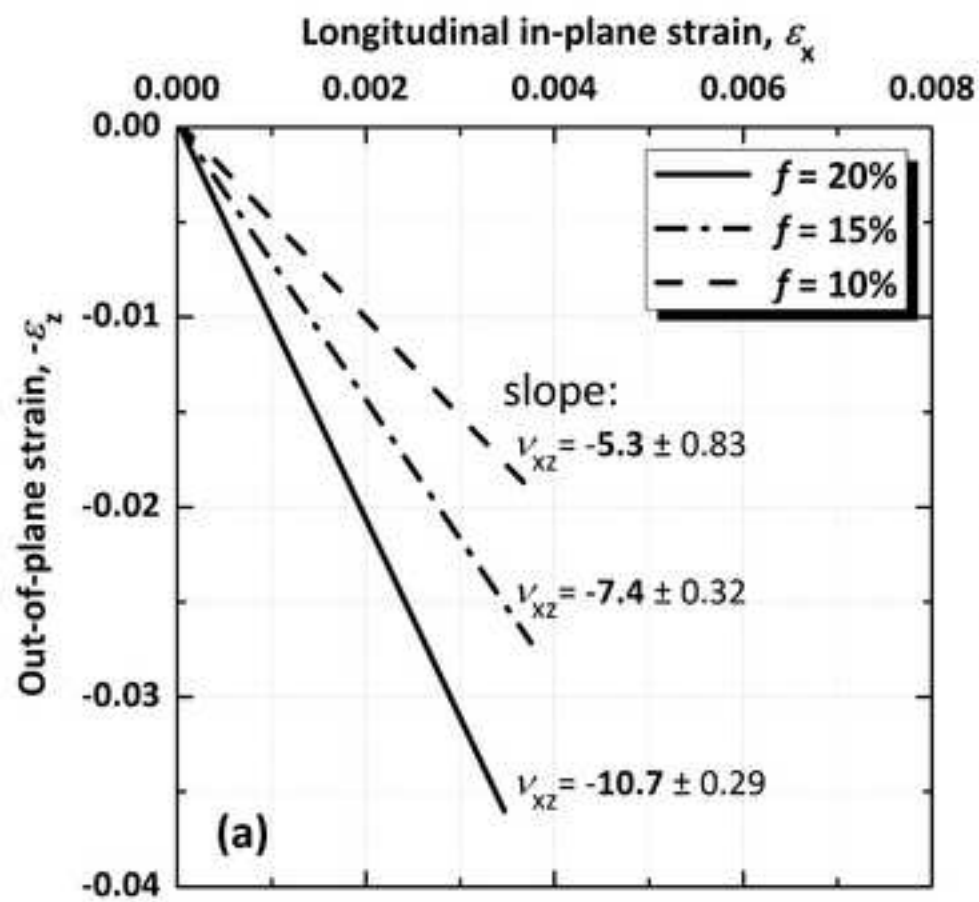
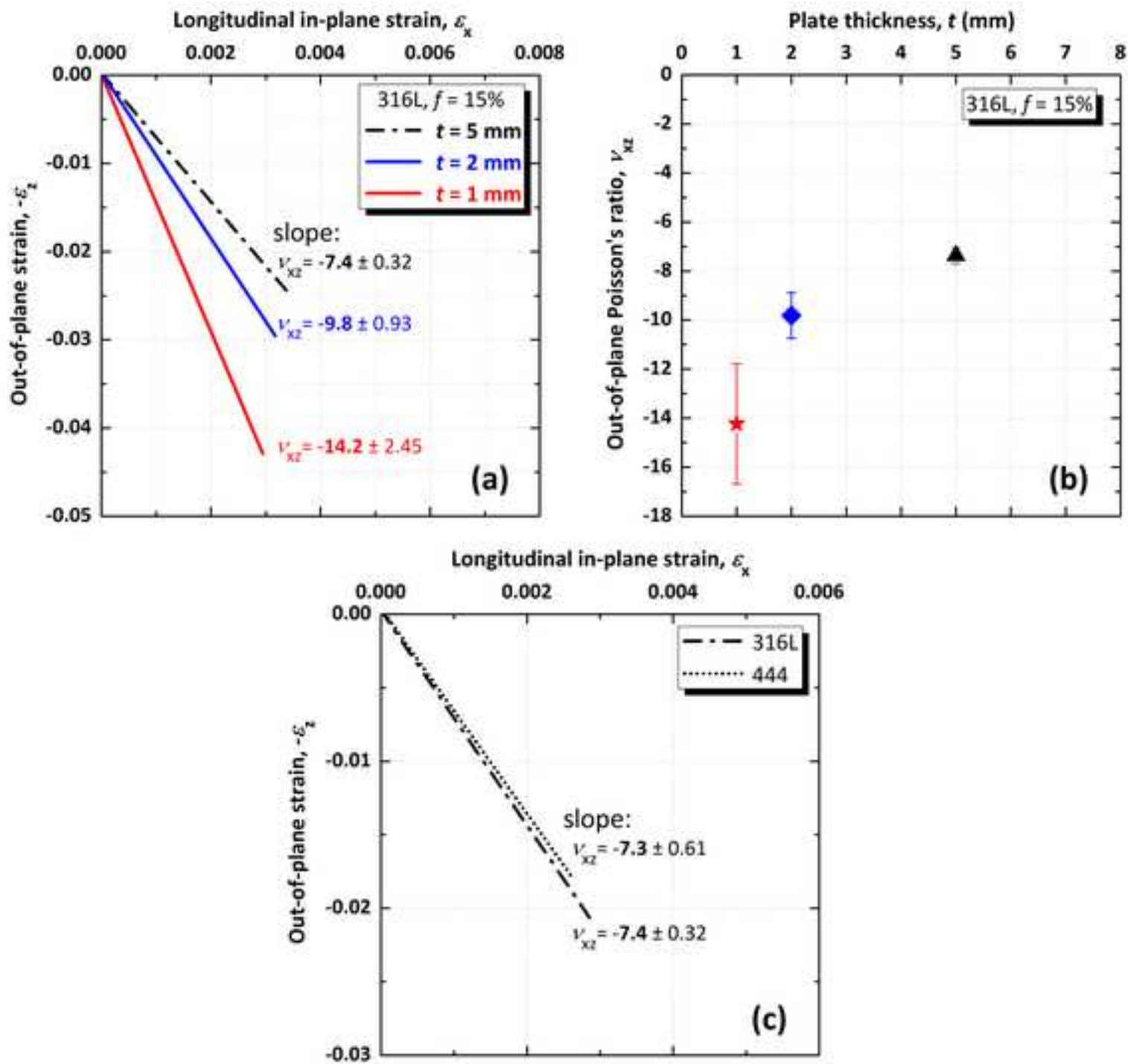


Figure 4
[Click here to download high resolution image](#)



Supplementary Material

[Click here to download Supplementary Material: 316L_90%porous_elastic_response.avi](#)